scientific reports

Check for updates

OPEN

Characterization of odor markers associated with aging in old ICR mice

Ji Eun Kim[1,2], Tae Ryeol Kim[1,2], Eun Seo Park[1], Ki Ho Park[1], Hee Jin Song[1], Ayun Seol[1], Su Jeong Lim[1], Su Ha Wang[1] & Dae Youn Hwang[1]✉

To identify and characterize the novel odor markers associated with aging in mice, alterations in the concentration of odorants in the urine, expression of metabolic enzymes, the histopathological structure of the sweat glands, and the expression of regulatory factors in sweat secretion were analyzed in ICR mice of four different ages (2, 6, 8 and 10-month-old). The concentrations of 15 odorants including ethylenimine and trimethylamine (TMA), and total volatile organic compounds (VOCs) were significantly higher in the urine of 8- and 10-month-old ICR mice. Among them, TMA was selected as an important odor biomarker associated with aging based on the aging-related upregulation and its odor characteristics. Also, the increase in TMA concentrations was reflected in the transcription levels of the gene encoding TMA monooxygenase in the livers and the feet as well as an age-dependent increase in the lumen area and secretory coiled portion of the sweat glands of mice. These results provide novel scientific evidence that the age-dependent changes in the volatiles in the urine are indicative of aging-related odors in ICR mice. Specifically, the study shows that TMA has potential as a novel diagnostic odor biomarker associated with aging in ICR mice to establish experimental animal platform for analyzing the efficacy and action mechanism of deodorants.

Keywords Aging, Odor, VOCs, Trimethylamine, Sweat gland

The characteristic body odor associated with older individuals is often referred to as the 'old person smell', or 'nursing home smell'[1]. This odor is produced due to age-dependent changes that result in the release of odorous substances from the skin glands, although it could be affected by bacterial activity, genetic features, and behavior[2–4]. Specifically, the complex mixture of lipid and fatty acids from the sebaceous glands are the fundamental sources of the 'old person smell' because the functional activity of this gland decreases in elders[5–7]. Also, a similar change in age-dependent loss of functionality has been detected in the apocrine glands[5]. To date, several odorants have been identified and serve as markers with a positive correlation between the extent of body odor and aging. It has been found that the quantum of the compounds, 2-nonenal and 2-nonanol was significantly increased by the oxidative degradation of ω7 unsaturated fatty acid in the elderly compared to the youth[7,8]. Other odorants identified include dimethyl sulfone, benzothiazole, aldehyde, and nonanal which also show similar age-dependent increases[7]. Furthermore, some significant differences were detected in the level of pleasantness and intensity of body odor between the elderly and the youth[1]. However, most of the studies on the identification and characterization of age-associated odors have been conducted only on humans. Few studies in the field of identifying volatiles that exhibit age-specific changes in urine are being conducted in animal experiments[9,10]. Actually, the direct studies for the evaluation of deodorants efficacy and identification of odor marker on humans has many limitations although the demand for studies on the identification and action mechanism of materials for deodorants continues to enhancement[9]. This is because the body odors of human are affected by various factors such as genetics, diet, medications and hygiene, and these properties have majorly contributed to produce the derivation of very wide-ranging data and inconsistent results for them[10]. Therefore, the establishment of an analysis platform based on new odorous marker using experimental animal that are bred under the consistent condition is crucial to enable repetitive and meticulous evaluation of potential candidates with deodorants activity.

Age-related alterations in body odor have been analyzed in several animals, including mice, rabbits, and monkeys. Most of the studies have been carried out on mice because of their physiological similarity to humans,

[1]Department of Biomaterials Science (BK21 FOUR Program), Laboratory Animal Resources Center, Life and Industry Convergence Research Institute, College of Natural Resources and Life Science, Pusan National University, Miryang 50463, Republic of Korea. [2]Ji Eun Kim and Tae Ryeol Kim contributed equally to this work. ✉email: dyhwang@pusan.ac.kr

large litter size, short life span, and ease of breeding[11]. Also, they were analyzed the urine sample to detected age-related alterations in body odor due to a characteristic body odor of mice is derived from their urine and scent glands as well as the tissue structure of mouse skin different from that of humans[12,13]. The quantitative changes in the aging patterns in the urine vapor of C57BL/6J mice were first compared in mice between 12 and 23 months of age using gas chromatography-mass spectrometry (GC–MS), and their physiological age was successfully reflected in the chromatogram of their urine vapor[14]. Also, two urinary volatiles associated with age were identified in C57BL/6J-H-2k mice of different ages: adult (3–10 months old) and old (more than 17 months old). The amount of 2-phenylactamide was remarkably increased in the old group, while those of methylbutyric acids were decreased in the same group[15]. Four attractive volatiles including 3,4-dehydro-exo-brevicomin (DB), 2-sec-butyl-4,5-dihydrothiazole (BT), 2-isopropyl-4,5-dihydrothiazole (IT) and 6-hydroxy-6-methyl-3-heptanone (HMH) were identified to be responsible for the odors associated with aging in the urine of the C57BL/6J mice[16]. Furthermore, significant changes in the concentration of trimethylamine (TMA) were detected in the urine of ICR mice between 2 and 10 months of age[17]. However, insufficient scientific data exists to characterize the novel odor biomarkers associated with aging in mice.

To investigate the novel odor markers associated with aging in ICR mice as part of a study to establish an experimental animal platform for the efficacy analysis and action mechanism research of deodorants based on odorous marker, this study analyzed the concentration of odorants in the urine, the transcriptional levels of genes encoding metabolic enzymes, the histopathological structure of the sweat glands, and the transcriptional levels of the functional regulators in sweat secretion. Thus, our study will be provided a novel system that can investigate the action mechanism and efficiency of deodorants based on newly identified odor biomarkers.

Results

Verifying the age of ICR mice in four different groups

First, we analyzed the appearance, body weight, telomere length, and ammonia concentrations of the ICR mice in the four groups to verify the aging of the mice in each group. The body size, weight and morphology gradually increased from 2 months to 10 months of age, while the telomere length decreased within each group (Fig. 1A). Also, the concentration of ammonia in the dirty bedding significantly increased only in the 8- and 10-month-old group compared to 2- and 6-month-old groups ($p < 0.001$). During the entire experimental period, the ammonia concentrations increased from day 3 to day 5 ($p < 0.001$), although the concentrations were highest in the dirty bedding of the 10-month-old group. However, the ammonia levels were maintained at a constant level during the first two days (Fig. 1B). These results suggested that the mice in the four different age groups used in this study were suitable for the characterization of age-related odors.

Identification of odor markers associated with aging in the urine of ICR mice

To identify the odor markers associated with aging in the ICR mice, alterations in the concentration of odorants were measured in the urine samples obtained from 2-, 6-, 8- and 10-month-old ICR mice using comparative gas chromatography-mass spectrometry (GC–MS) analysis. Significant peak changes in the GC–MS chromatogram of the urine were detected in the 8- and 10-month-old ICR mice when compared with the 2- and 6-month-old mice (Fig. 2A). A total of fifteen peaks including those for ethylenimine, TMA, benzene, N,N, N',N'-tetramethylmethanediamine (TMMA), toluene, phenylethyne, styrene, azulene, biphenyl, diphenylmethane, 1,4-dihydrodibenzofuran, dibenzofuran, 3-hydroxybiphenyl significantly increased in an age-dependent manner, although they involved few unknown compound (Fig. 2B). Also, the relative levels of the total VOCs significantly increased with age in the ICR mice, while the highest level was detected in the 10-month-old mice. However, these VOC levels were maintained at a constant level in the 2- and 6-month-old mice (Fig. 2C). Also, the principal component analysis (PCA) score plot showed compounds detected by GC–MS analysis were successfully clustered based on the age of mice (Fig. 2D). Among the fifteen compounds, three compounds including TMA, ethylenimine, and methanediamine were selected as candidates for odor markers associated with aging since evidences of their scientific potential as odorous substances has been reported[18]. The concentrations of TMA and ethylenimine remarkably increased in an age-dependent manner ($p < 0.001$), although the highest levels were measured in the 8-month-old mice (Fig. 3A and B). A similar pattern was detected in the concentrations of methanediamine. However, the levels were remarkably higher in the 10-month-old mice when compared with the 8-month-old mice ($p < 0.001$) (Fig. 3C). Therefore, these results suggest that TMA, ethylenimine, and methanediamine may be considered odor markers associated with aging in ICR mice.

Alterations in the expression of genes encoding TMA monooxygenase during age-dependent increases in TMA concentrations

Next, we selected TMA as the key odor biomarker associated with aging because, in an earlier study, it was observed that its concentration was 11.7-fold higher in the 10-month-old ICR mice than in the 2-month-old ICR mice[17]. Also, this selection was supported by the fact that this study revealed that TMA concentrations increase the most during aging. To determine whether the increases in TMA concentrations were accompanied by changes in the expression of the gene encoding the enzyme TMA monooxygenase (flavin-containing monooxygenase 3, *FMO3*), which converts odorous TMA into non-odorous trimethylamine N-oxide (TMAO), the transcription levels of the gene encoding it were analyzed in the liver and feet of the ICR mice (Fig. 4A). In the liver tissue, the transcription levels of this gene gradually increased in an age-dependent manner from 2-month-old to 10-month-old mice ($p < 0.001$). Also, a similar pattern was observed in the foot tissues, although the highest level was detected in 8-month-old mice ($p = 0.003$) (Fig. 4B). Therefore, these results show that the increases in the TMA concentrations may be associated with alterations in the expression levels of *FMO3* in the liver and foot tissues of the ICR mice.

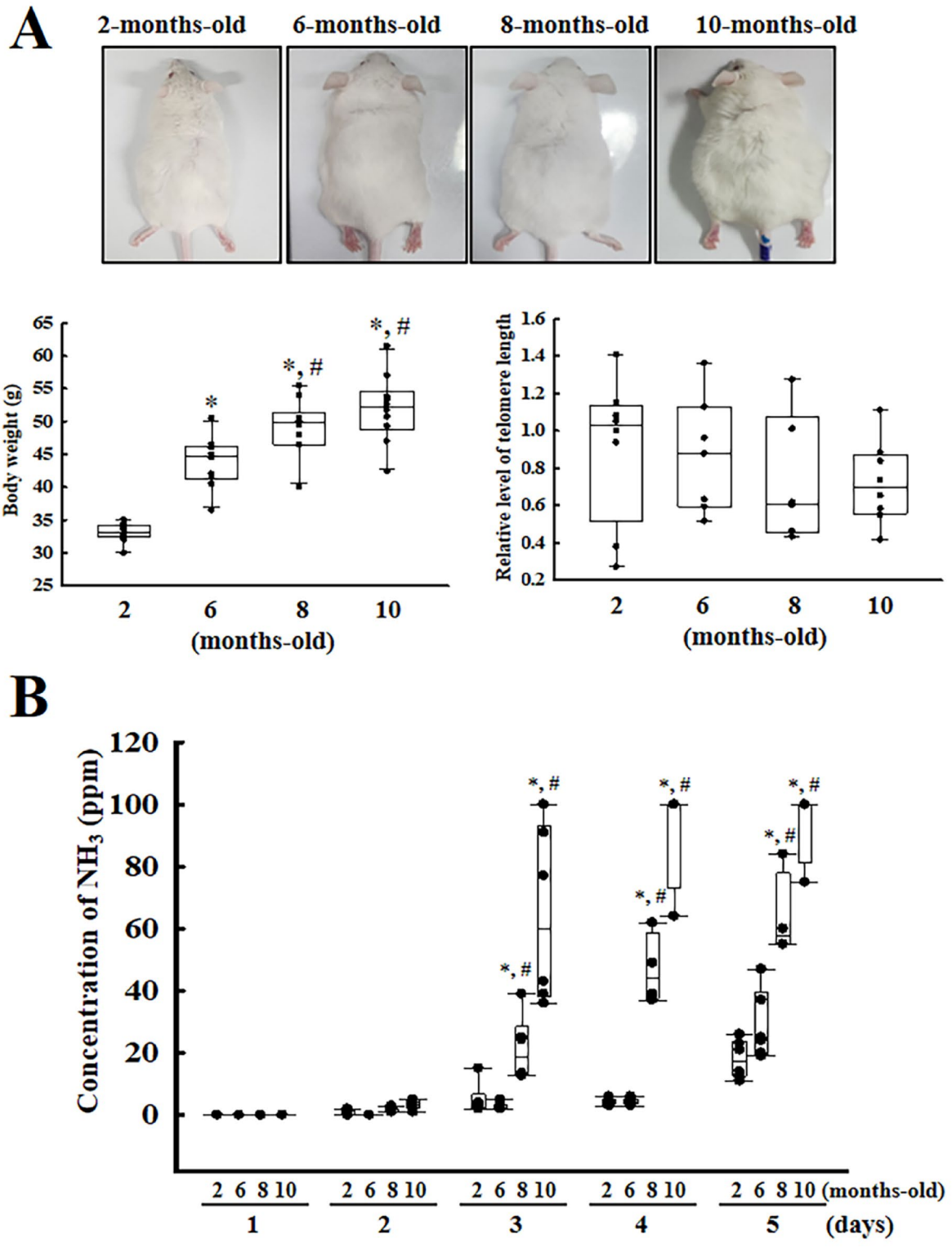

Fig. 1. Obeservation of the aging in ICR mice. (**A**) Appearance, body weight and telomere length. All the mice were photographed with a digital camera and their weight were measured using electrical balance. The images of mice were represented are presented as animals with average weight in each group. The total genomic DNAs were collected from the liver tissues of five to six mice per group and the length of the telomeres was analyzed twice for each mouse. (**B**) Ammonia concentrations in dirty bedding. The ammonia concentration was measured in dirty bedding obtained from a single ICR mouse, as described in the 'Materials and Methods' section. Three to five mice per group were used to prepare the dirty bedding, and the ammonia concentrations were assayed in duplicate for each bedding. The data are reported as the means ± SD. $^{*}p < 0.05$ compared with the 2-month-old group. $^{\#}p < 0.05$ compared with the 6-month-old group.

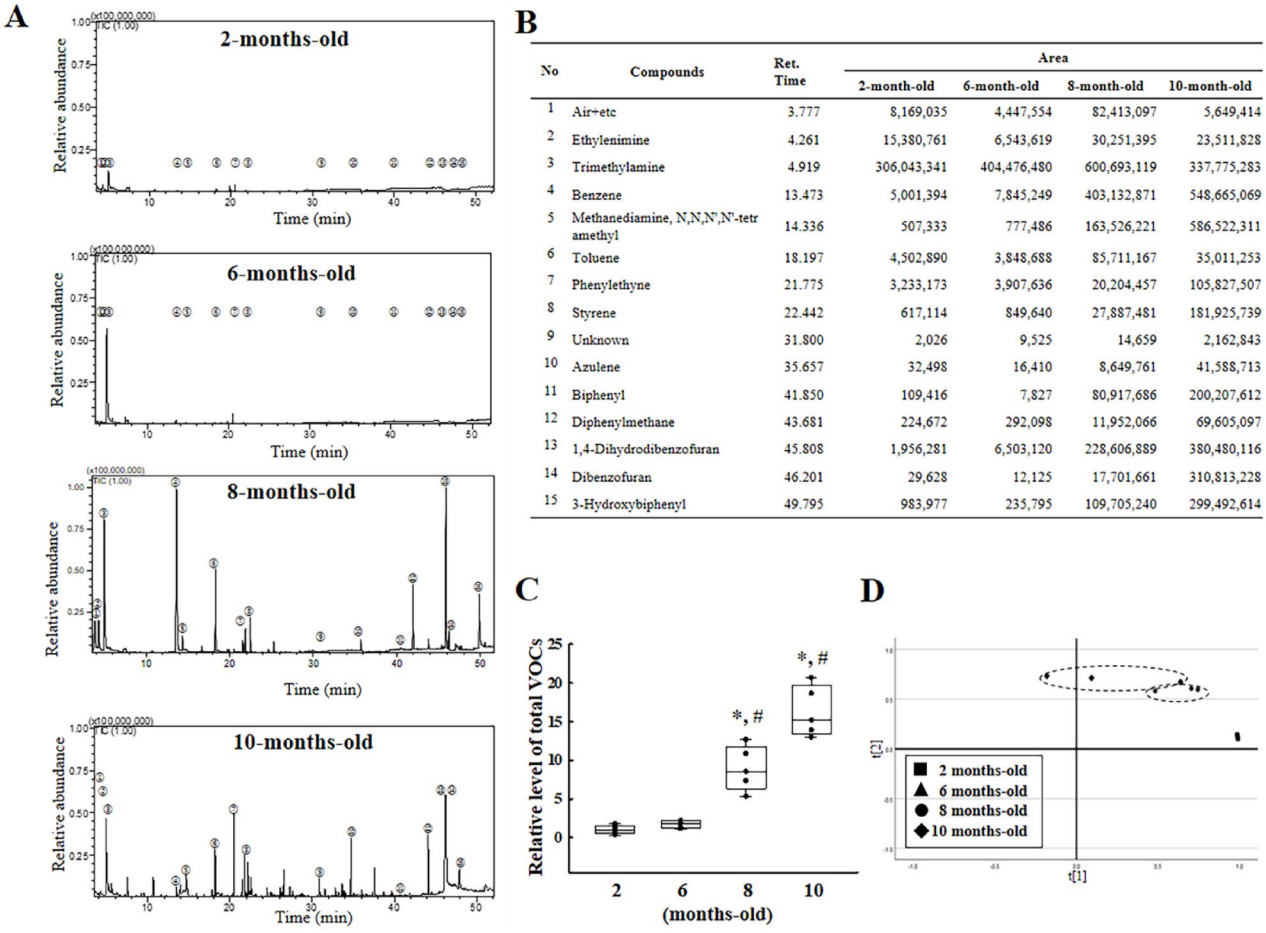

No	Compounds	Ret. Time	Area			
			2-month-old	6-month-old	8-month-old	10-month-old
1	Air+etc	3.777	8,169,035	4,447,554	82,413,097	5,649,414
2	Ethylenimine	4.261	15,380,761	6,543,619	30,251,395	23,511,828
3	Trimethylamine	4.919	306,043,341	404,476,480	600,693,119	337,775,283
4	Benzene	13.473	5,001,394	7,845,249	403,132,871	548,665,069
5	Methanediamine, N,N,N',N'-tetr amethyl	14.336	507,333	777,486	163,526,221	586,522,311
6	Toluene	18.197	4,502,890	3,848,688	85,711,167	35,011,253
7	Phenylethyne	21.775	3,233,173	3,907,636	20,204,457	105,827,507
8	Styrene	22.442	617,114	849,640	27,887,481	181,925,739
9	Unknown	31.800	2,026	9,525	14,659	2,162,843
10	Azulene	35.657	32,498	16,410	8,649,761	41,588,713
11	Biphenyl	41.850	109,416	7,827	80,917,686	200,207,612
12	Diphenylmethane	43.681	224,672	292,098	11,952,066	69,605,097
13	1,4-Dihydrodibenzofuran	45.808	1,956,281	6,503,120	228,606,889	380,480,116
14	Dibenzofuran	46.201	29,628	12,125	17,701,661	310,813,228
15	3-Hydroxybiphenyl	49.795	983,977	235,795	109,705,240	299,492,614

Fig. 2. GC–MS chromatograms and list of the major volatile components in the urine samples from 2, 6, 8, and 10-month-old ICR mice. (**A**) Chromatograms. Each peak refers to the compounds mentioned in the table below. The volatile compounds were identified by comparing the MS spectrum and RIs of the components in the EHF with the known authentic standards available in the NIST library (2005). (**B**) Peak area of 15 compounds showing significant differences between the four different age groups. (**C**) Total VOC levels in the 2-, 6-, 8- and 10-month-old mice. (**D**) PCA score plot. 8- and10-month-old group were clustered with different dotted circle. The urine samples were collected from three to five mice per group and the GC–MS analyses were performed twice for each mouse. The data are reported as the means ± SD. $^{*}p < 0.05$ compared with the 2-month-old group. $^{\#}p < 0.05$ compared with the 6-month-old group. Abbreviations: GC–MS: Gas chromatography-mass spectroscopy, RIs: retention indices, EHF: extremely high frequency, NIST: National Institute of Standards and Technology, VOCs: volatile organic compounds, PCA: Principal component analysis.

Alterations in the histological structure and function of the sweat glands during aging

Finally, we tried to investigate whether the alteration in the concentration of the odorants associated with aging in the urine is accompanied by changes of them in sweat because urine and sweat are main waste products from the body and the cause of characteristics body odor. However, collecting sweat from mice bred in bedding cage is technically very difficult and limited. Therefore, we analyzed the only histological structure and function of sweat glands instead of analyzing major components in sweat to overcome this problem. Hence, the alterations in the histological structure of the sweat glands and the transcription levels of the genes encoding the regulatory factors for sweat secretion were analyzed in the feet of 2-, 6-, 8- and 10-month-old mice. During the aging of the mice, significant alterations were detected in the hematoxylin and eosin (H&E)-stained section of the sweat glands. The lumen area and the secretory coil portions increased significantly in an age-dependent manner in 2-, 6-, 8- and 10-month-old mice ($p < 0.001$) (Fig. 5). Also, the above histological alterations in the feet of mice were partially accompanied by increases in the transcription levels of the genes encoding the regulatory factors for sweat secretion. The transcription levels of the Na-K-ATPase (NKA), aquaporin 5 (AQP5), and forkhead box protein A1 (FOXA1) genes were gradually enhanced in 8 or 10-month-old mice compared to 2 or 6-month-old mice ($p = 0.002$) even though the variation was large (Fig. 6). Therefore, these findings show the possibility that alterations in the concentration of odorants associated with aging in the urine may be linked to these changes of the odorants in sweat of the ICR mice.

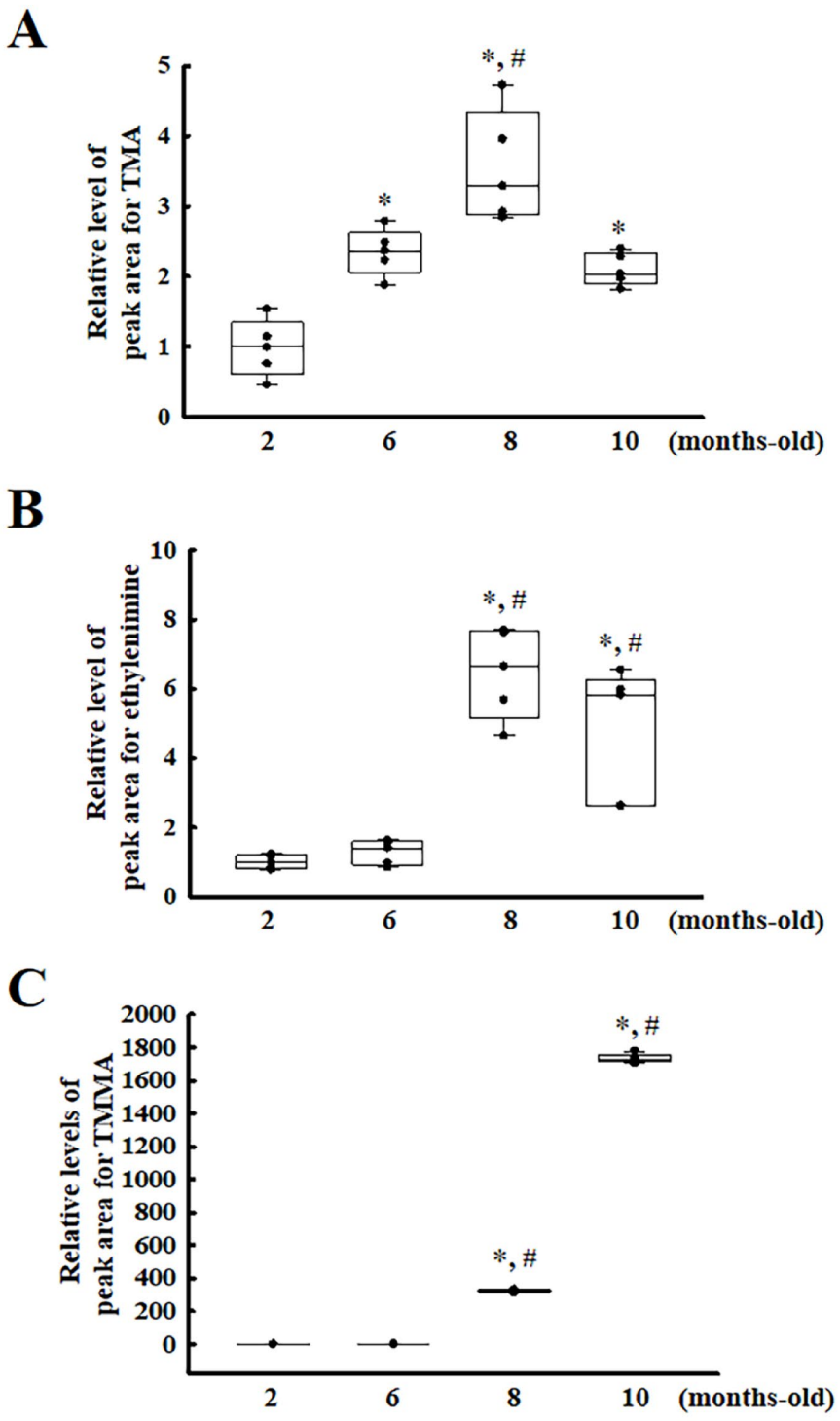

Fig. 3. Peak area of the three amine compounds detected in the urine of mice aged 2, 6, 8, and 10 months. The peak areas for TMA (**A**), ethylenimine (**B**), and TMMA (**C**) were presented as a relative level. The urine samples were collected from three to five mice per group, the GC–MS analyses were performed twice for each mouse. The data are reported as the means ± SD. $^{*}p < 0.05$ compared with the 2-month-old group. $^{\#}p < 0.05$ compared with the 6-month-old group. Abbreviations: GC–MS: Gas chromatography-mass spectroscopy, TMA: Trimethylamine, TMMA: N,N, N',N'-tetramethylmethanediamine.

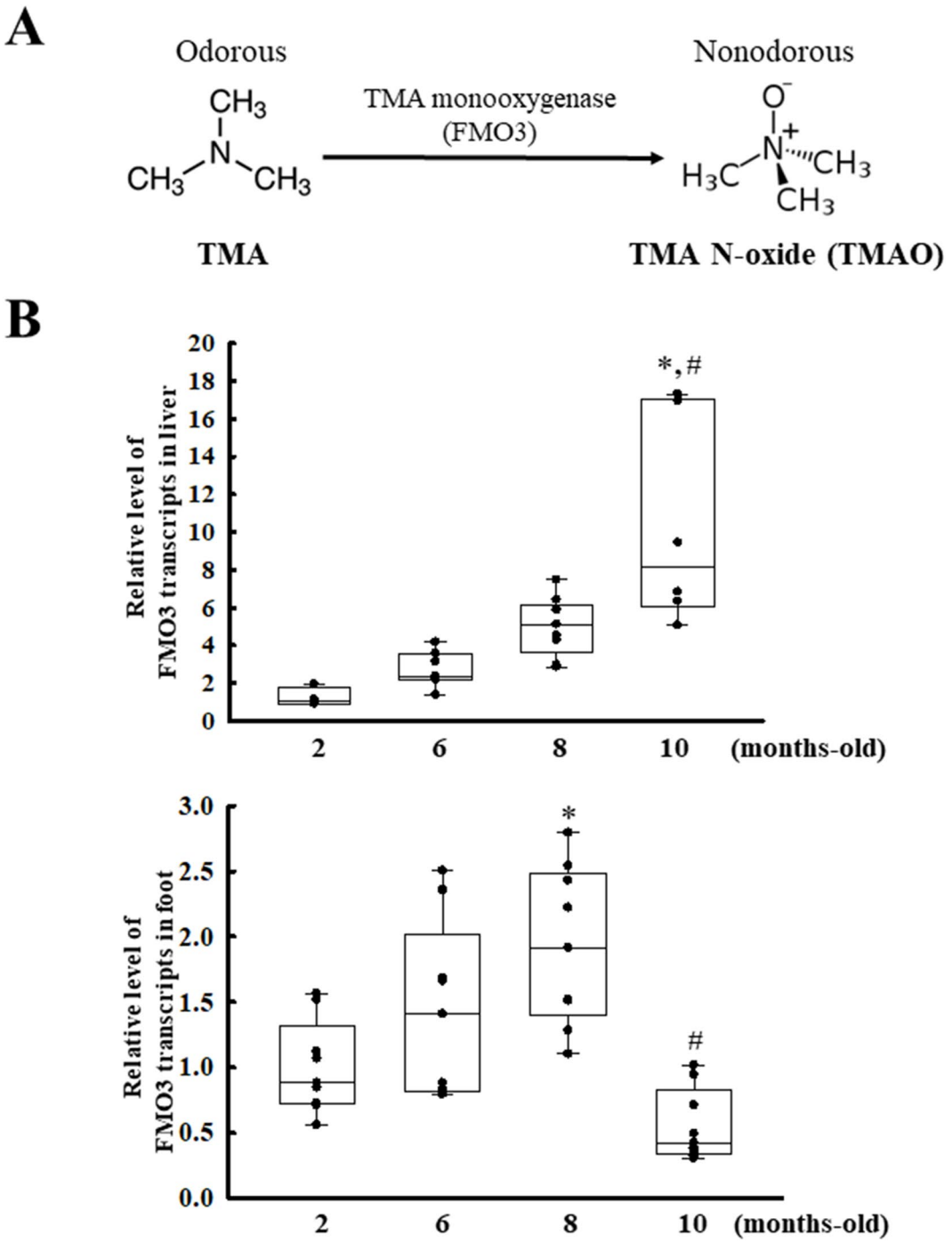

Fig. 4. Transcription level of the gene encoding TMA metabolic enzyme. (**A**) Biochemical reaction of TMA. This compound was catalyzed into TMAO through TMA monooxygenase (FMO3). (**B**) Transcript levels of gene encoding FMO3. After purifying the total mRNA of the liver and foot tissue, transcription levels of this gene were detected by qRT-PCR analysis using specific primers. The preparation of the total RNAs from the liver and feet tissues was performed on three to five mice per group, and the levels of the PCR product were analyzed twice for each sample. The data represents the means ± SD. $^{*}p < 0.05$ compared with the 2-months-old group. $^{\#}p < 0.05$ compared with the 6-month-old group. Abbreviations: TMA: Trimethylamine, TMAO: Trimethylamine N-oxide, FMO3: Flavin-containing monooxygenase 3.

Discussion

The elderly suffers from the 'old person smell' and this has been receiving a lot of attention as it can cause severe embarrassment during social interactions[19]. Research to characterize the novel odor compounds associated with aging can aid the development of suitable deodorants. In this study, we analyzed the concentrations of the odor components of urine, transcription levels of the genes encoding the metabolic enzymes, the histological

A

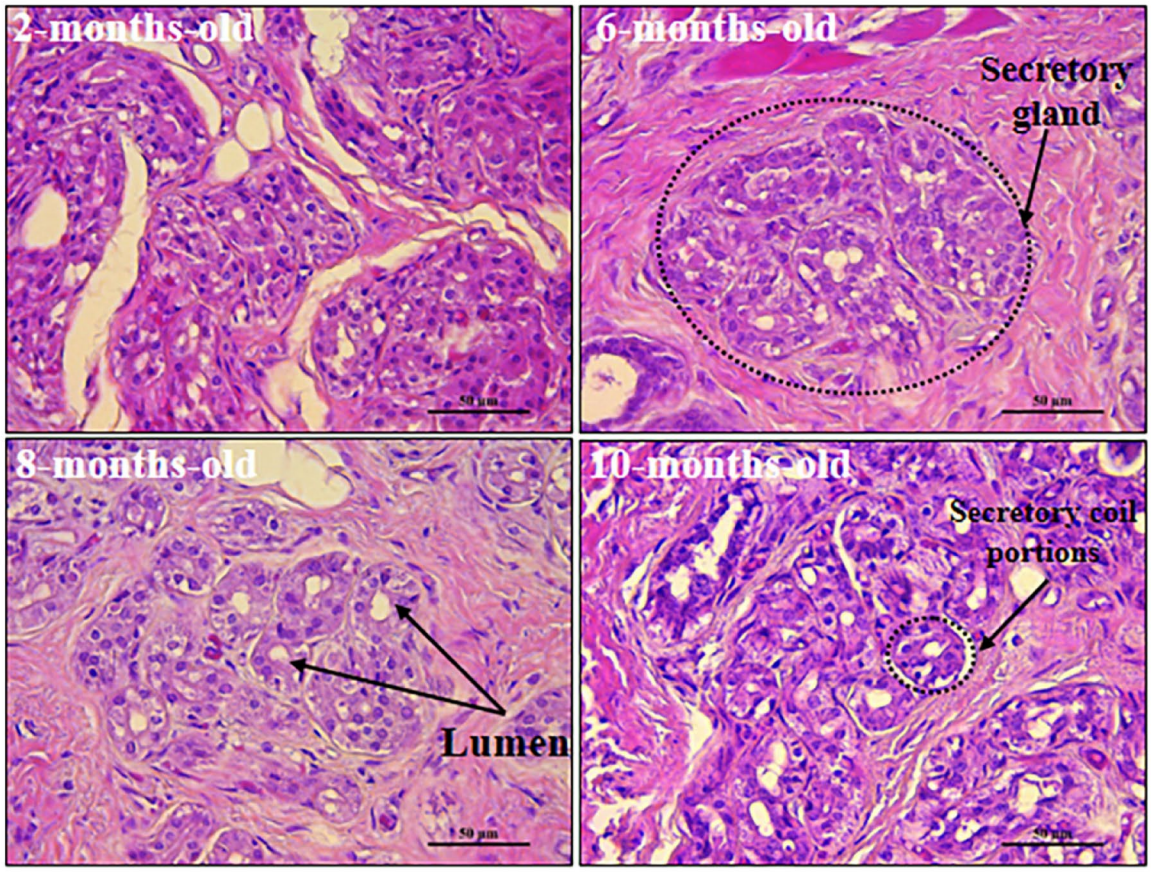

B

Group	Lumen area (μm²)	Secretory coil portions (μm²)
2-months-old	29.77±2.48	700.59±40.70
6-months-old	48.27±11.93*	841.60±107.63
8-months-old	82.65±11.64*,#	914.63±63.26*
10-months-old	85.93±6.53*,#	934.12±77.90*

Fig. 5. Histological structure of the sweat glands in mouse feet. (**A**) Histopathological structure of the sweat gland. These structures were observed in H&E-stained foot sections of ICR mice at 400× magnifications. (**B**) Histopathological characteristics. The size of the lumen area and secretory coil portions was determined using the Leica Application Suite. Three to five mice per group were used to prepare the foot sections, and the size of the gland tubule and lumen in sweat glands was counted in duplicate for each section. The data are reported as the means ± SD. $^{*}p < 0.05$ compared with the 2-month-old group. $^{\#}p < 0.05$ compared with the 6-month-old group. Abbreviations: H&E; Hematoxylin and eosin.

structure of the sweat glands, and the transcription levels of the genes encoding the regulatory factors associated with gland secretion to characterize novel odor markers in ICR mice of four different age groups. These results suggest the possibility that several odor compounds, including ethylenimine, TMA, and TMMA, may be considered age-dependent markers of the 'old person smell'. These odor markers will be contributed to the establishment of the experimental platform to investigate the efficacy and action mechanism of deodorants. However, further research is needed with respect to the molecular mechanism of odor production.

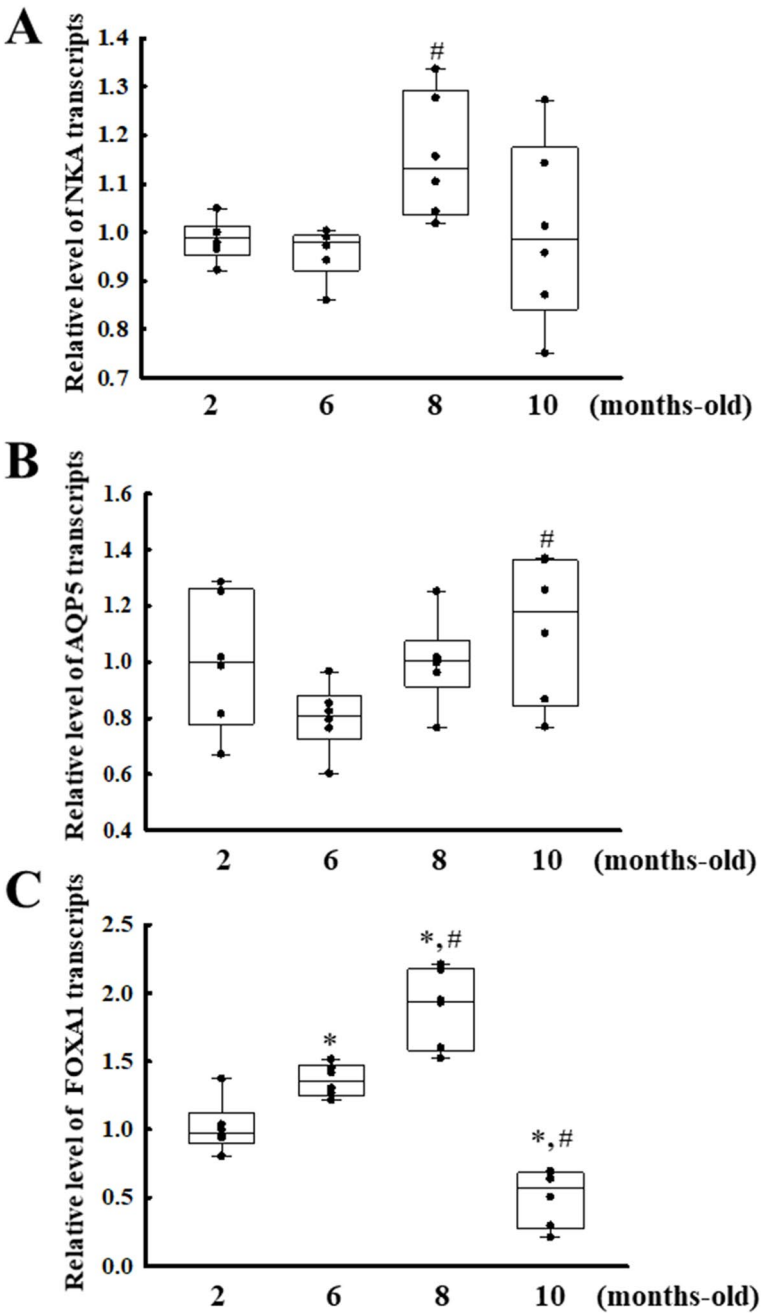

Fig. 6. Transcription levels of the genes encoding metabolic enzymes for sweat secretion. The transcript levels of genes (**A**) NKA, (**B**) AQP5, and (**C**) FOXA1 were detected in the total mRNA of the feet tissue by RT-qPCR analysis using specific primers. The preparation of the total RNAs from the foot tissues was performed on three to five mice per group, and the levels of the PCR product were analyzed twice for each sample. The data represents the means ± SD. $^{*}p < 0.05$ compared with the 2-month-old group. $^{\#}p < 0.05$ compared with the 6-month-old group. Abbreviations: NKA: Na-K-ATPase, AQP5:aquaporin 5, FOXA: forkhead boxa1.

Age-dependent changes in body odors have been investigated in the urine volatiles of only two different mice strains, although the ages of the animals used in the analysis varied. In the C57BL/6J mice, six different odor compounds were identified by GC–MS analyses. Among them, significant differences in the concentrations of the 2-phenylacetamide and methylbutyric acids were detected between mice aged 3–10 and 17–21 months. The concentration of 2-phenylacetamide was higher, but that of the methylbutyric acids was lower in old mice than in young mice[15]. The 2-phenylacetamide is known as a metabolite of L-phenylalanine, and this increase pattern of this compound may link to alterations on the metabolism of serum phenylalanine concentration because it is associated with potentially with the aging process[20,21]. Also, this change of methylbutyric acids is thought to be due the potential effect on vascular calcification[22]. A similar pattern in the concentrations of 3,4-dehydro-exo-brevicomin (DB), 2-sec-butyl-4,5-dihydrothiazole (BT), and 2-isopropyl-4,5-dihydrothiazole (IT) and

6-hydroxy-6-methyl-3-heptanone (HMH) derivatives was detected in the old group (28 months-old) compared to the adult (3–8 months-old) and the aged group (15–20 months-old) of C57BL/6 mice. The concentrations of DB, BT, and IT were increased in old mice, while that of 3HMH derivatives was decreased in the same group[16]. Among them, DB, BT and IT are one of enantiomeric compounds and pheromones of male mouse for their chemical communications[23,24]. Also, HMH is a unique urinary constituent as one of active pheromones in male and female of three different mouse strains including BALB/c, CF-1, ICR/Aib and SJL/J x SWR/J F1, and has puberty-acceleration activity[25]. However, several different odorants were detected in the ICR mice. Sixteen odorants showed an increased concentration in the 10-month-old group compared to the 2-month-old group. Among them, TMA showed maximum differences in urine concentrations between the 2- and 10-month-old mice[17]. In the present study, we identified fifteen odorants with variable urine concentrations in four different age groups of ICR mice. Among them, three amines (ethylenimine, TMA, and TMMA) were selected as age-related odorants based on their chemical properties. But, our study did not detect previously detected age-related odor compounds including 2-phenylacetamide, methylbutyric acids, DB, BT, IT and HMH. Most of the odorants identified in our results did not match those identified in previous studies. Only two odor compounds, namely TMA and benzene, have been detected both in our study and in a previous study comparing 2- and 10-month-old ICR mice[17]. Specifically, the differences in the composition of the odor compounds between the ICR mice and the C57BL/6 mice may be attributed to differences in the hereditary features, diet variety, breeding environments and hygiene condition although it is difficult to predict the exact cause. Therefore, the results of the present study provide important information on the profile of the urine volatiles associated with aging in ICR mice that should be considered during the identification of age-dependent odors. However, a brevicomine and thiazoline known as male pheromones were not detected in our study although male was used. The exact cause of the non-detection of these compounds needs to be considered for further study.

Meanwhile, the present study identified three amine compounds (TMA, ethylenimine, and TMMA) associated with aging in ICR mice. Their concentrations were remarkably increased in the urine of the two elder groups (8- and 10-month old) compared to two younger groups (2- and 6-month old). TMA has a smell similar to ammonia, even though it has a fishy odor at low concentrations[26]. Alterations in the concentration of this compound are closely related to various physiological or pathological metabolic processes in the body. During the development of trimethylaminuria (fish odor syndrome), the excess TMA is metabolized to TMAO in the liver tissue[27,28]. Also, the transcription level of TMA metabolic enzyme, FMO3, which is the most abundant one of FMO family members in the liver of human, were completely reflected in the age-dependent changes of TMA concentration to the age of 10-month-old[29]. The analyses for the concentration of TMA and the transcription of FMO3 in the liver of mice over 10-month-old of age will be needed as further studies to prove the correlation between these factors and age. However, the change of FMO3 levels in the liver tissue were partially consistent in those of foot tissue. This increase in FMO3 level was observed only up to 8-month-old mice but rather decreased at 10-month-old. This difference is thought to be contributed by the differential developmental and tissue-specific expression pattern of FMO genes[29–31].

Similar changes were detected in the odor associated with several pathogenic infections, bad breath, and bacterial vaginosis in the human body[26]. Specifically, TMA was associated with age-related odor in an evaluation study of the deodorizing effects of *Saccharina japonica* in 10-month-old ICR mice[17]. The results of the present study provide additional scientific evidence to correlate TMA with aging-related odor. In addition, ethylenimine causes severe inflammation of the respiratory tract, although it is a part of various polymerization products, binders, and adhesives[32]. This compound is well known to have an ammonia-like odor and its threshold is 2 ppm in air[33,34]. The hydrochloride of TMMA has been widely used in chemical synthesis and amide synthesis because its simple form can only exist transiently in solution[35,36]. Specifically, TMMA plays an important intermediate role during the abiogenesis of heterocyclic compounds[37]. However, there has been no reported correlation between the above two TMA related compounds and body odors to date. The results of the present study provide the first scientific evidence that ethylenimine and TMMA may be considered novel age-related odorants.

Sweat glands are exocrine glands that play an important role in several physiological functions, including the maintenance of body temperature, waste excretion, sweat secretion, and inhibition of bacterial growth[38,39]. They are distributed throughout the whole-body surface, although the apocrine sweat glands are mainly found in the armpits, groin, and nipples. Also, sweat glands comprise a secretory unit and a duct unit that has a narrow lumen and is responsible for the production of body odor[40]. Among the two types of sweat glands, the apocrine sweat glands are the main cause ofbody odor in humans, although mice also have specialized forms of apocrine sweat glands[41]. In the present study, we analyzed the histological structure and functions of the sweat glands in the feet of ICR mice of four different age groups because it was technically impossible to analyze odor components in sweat of mice to investigate whether age-related changes in the urine odorants are accompanied by changes of sweat odorants. The old age groups including 8- and 10-month-old mice showed significant alterations in the secretory glands and the lumen of the H&E-stained foot section as well as transcription levels of three functional genes including the FOXA1, NKA, and AQP5 genes in the total RNA from the foot. Among these genes, FOXA1 is well known to have function in the development and differentiation of secretory coil-like structures and the secretory function of the 3D reconstructed eccrine sweat glands[42,43]. NKA play an important role in the regulation of sweating, while AQP5 has the function for the regulation of the sweat secretion rate[44,45]. These results provide the first scientific evidence that the production of several urine odorants associated with age may be linked to the age-related changes of odorants in sweat of ICR mice although only changes in the histological structure and functions of the sweat gland in the foot were presented as indirect evidence. However, more studies are required to identify and characterize the novel odorants associated with aging among the various components in the sweat secreted by the sweat glands.

In summation, the present study characterized the novel odorants associated with aging in ICR mice of four different age groups through GC–MS, histological, and RT-qPCR analyses. Our results provide novel

evidence that the increase in the TMA, ethylenimine, and TMMA concentrations is tightly correlated with the aging of ICR mice. Also, the results for structural and functional changes in the sweat glands in the feet were indirectly show the correlation between alterations in the urine odorants and those in sweat of mice. Therefore, our findings suggest that TMA could be considered one of the novel odor markers associated with aging in ICR mice, and this novel marker will greatly contribute to establishing an important first step in the experimental animal platform for deodorant analysis. However, the present study has a few limitations as follows: The study did not analyze the odor compounds in the urine of older mice over 10 months of age and does not provide any data for a direct correlation between the odor compounds in the urine and sweat in the production of age-related odors. Thus, our results and additional studies on experimental animal platform for deodorant analysis could greatly contribute to the identification and evaluation of various materials that can reduce and prevent the odors associated with aging.

Methods

Design of the animal experiment

All experimental and analytical methods were performed in accordance with relevant guideline and regulations. Also, our experiments complied with the Animal Research: Reporting of In Vivo experiments (ARRIVE) guidelines. The animal experiment protocol was approved by the Pusan National University-Institutional Animal Care and Use Committee (PNU-IACUC) based on ethical procedures for scientific care (Approval Number PNU-2023-0330). All the ICR mice (male) were bred at the Pusan National University-Laboratory Animal Resources Center, accredited by the Ministry of Food and Drug Safety (KFDA) (Accredited Unit Number-000231) and the Association for Assessment and Accreditation of Laboratory Animal Care (AAALAC) International (Accredited Unit Number; 001525). They were obtained from the Samtako BioKorea Co. (Osan, Korea) and provided with a standard diet (Samtako Bio Korea Co., Osan, Korea) comprising crude protein (22.5%), fat (5.0%), fiber (4.5%), ash (6.5%), nitrogen-free extracts (50.5%) and moisture (11.0%). The mice were given access to filtered tap water *ad libitum*. The mice were maintained in a specific pathogen-free (SPF) state under a light-dark cycle (08:00 h to 20:00 h) at 22 ± 2℃ and relative humidity of 50 ± 10%.

Seven-week-old ICR mice ($n = 32$) were divided into four experimental subgroups based on age: the 2-month-old group ($n = 8$), 6-month-old group ($n = 8$), 8-month-old group ($n = 8$), and 10-month-old group ($n = 8$). When the animals in each group reached the appropriate age, the ammonia concentration in their dirty bedding was individual measured for 5 days, and the urine of each mouse was separately collected using an individual metabolic cage. Subsequently, these mice were euthanized by a trained researcher using an appropriate chamber with a gas regulator and CO_2 gas with a minimum purity of 99.0% based on the American Veterinary Medical Association (AVMA) Guidelines for the Euthanasia of Animals. A cage containing the mice was placed in the chamber, and CO_2 gas of 99.0% purity was introduced into the chamber without pre-charging, with a fill rate of ~ 50% of the chamber volume per minute. The euthanasia endpoint of the mice was confirmed by ascertaining cardiac and respiratory arrest, or dilated pupils and fixed bodies. The liver and foot tissues collected from the mice were used in histopathological analyses and molecular assay.

Measurement of body weight, size and morphology

The body weight of all mice in subset group were measured twice using electrical balance (Mettler Toledo, Greifensee, Switzerland) before autopsy. The average body weight of each group was calculated from the body weights of all mice within each group, and then the mice close to the average body weight were photographed with a digital camera (Canon, Middlesex, UK).

Analyses of telomere length by quantitative PCR

The length of the telomeres in the liver tissue of mice was quantified by qPCR as described in a previous study[46,47]. After chopping the frozen liver (25 mg) with scissors in mix solution (0.01 M NaCl, 0.05 M Tris, 0.2 mM ethylenediamine tetraacetic acid (EDTA), 0.173 mM sodium dodecyl sulfate (SDS)), the tissues were digested with 20 mg/mL of proteinase K (Carl Roth, Karlsruhe, Germany) at 56℃ overnight. The total genomic DNA was purified from the liver homogenates mixture using chloroform extraction. After quantification of the genomic DNA, the telomeres were amplified using a gDNA template, 2× Power SYBR Green (Toyobo Life Science, Osaka, Japan), and two specific primers for the telomere and single-copy reference gene (36b4); Forward and reverse primer for telomere, 5′-ACA CTA AGG TTT GGG TTT GGG TTT GGG TTT GGG TTA GTG T-3′ and 5′-TGT TAG GTA TCC CTA TCC CTA TCC CTA TCC CTA TCC CTA ACA-3′: Forward and reverse primer for 36b4 gene, 5′-ACT GGT CTA GGA CCC GAG AAG-3′ and 5′-TCA ATG GTG CCT CTG GAG ATT-3′. The optimal thermal program was one cycle at 95℃ for 10 min, two cycles, comprising one at 95℃ for 15 s and the second at 49℃ for 15 s, followed by 45 cycles at 95℃ for 15 s, 60℃ for 10 s, 72℃ for 15 s. Fluorescence intensities were measured at the end of each extension cycle. The telomere length was quantified relative to the level of 36b4, by comparing the cycle threshold (Ct) values at a consistency of fluorescence intensity[48].

Measurement of the ammonia concentration in dirty bedding

The ammonia concentration was measured in the dirty bedding of the breeding cage using the GasAlertMicro 5 multi gas detector (BW Technologies by Honeywell, Calgary, Canada). While breeding the mice in the wood chips for five days, the ammonia concentration on the surface of the dirty bedding was measured daily in duplicate. The blanks used a bedding cage without breeding the mice.

GC–MS analysis

The odorous compounds in the urine samples were identified using GC–MS analysis, which was performed using a slight modification of the methods described elsewhere[49]. Five drops of urine were harvested from each

mouse, and a supernatant was collected from the centrifuged sample. The urine samples (250 µL) from which the debris had been removed were dried at 60 °C for 30 min. The samples were absorbed into the tube at 100 mL per minute for five minutes. These tubes were analyzed by GC–MS (QP-2010 A, Shimadzu, Japan) equipped with an automatic thermal desorption apparatus (ATD 400, Perkin Elmer, UK). The AT-1 capillary column was 60 m × 0.32 mm × 1.0 µm, and the mass range was 20–350 m/z. The temperature ramp was in a programmed mode with an initial temperature of 35 °C held for 10 min, and then increased linearly from 35 °C to 120 °C at 8 °C/10min, from 120 °C to 180 °C at 12 °C/min, from 180 °C to 230 °C at 15 °C/min, and held at 230 °C for 10 min. The experimental mass spectra were compared with the data stored in the Wiley229, Nist21, and Nist107 Libraries to identify the GC traces of the odorant compounds in the urine metabolites. Duplicate samples were collected during each sampling process to assess the precision and reliability of theanalytical method. In addition, laboratory blanks (empty bottle) and pump calibrations were conducted before every sampling. The flow rate of the sampling pumps was calibrated using a mass flow meter before each sampling to ensure that the flow deviation was less than 5%. The calibration curve of the standard toluene was obtained by fitting the eight different concentration points (range of 0.003–0.2 µg) with $R2 > 0.99$. The relative proportions of the emitted odorants were semi-quantified as peak areas due to the limited availability of calibration gases for most of the individual odorants[50].

Quantitative real-time (qRT)-PCR analysis

The total RNA was purified from the liver and the foot using an RNA Bee solution (Tet-Test Inc., Friendswood, TX, USA) according to the manufacturer's instructions. After homogenization using a POLYTRON® PT-MR 3100 D Homogenizer (Kinematica AG, Lucerne, Switzerland), the total RNAs were harvested from the cell lysates by centrifugation at 10,000 × g for 15 min. The RNA concentration was determined using a Nano-300 Micro-Spectrophotometer (Allsheng Instruments Co. Ltd., Hangzhou, China). The total complementary DNA (cDNA) was synthesized against mRNA (4 µg) using 200 units of Superscript II Reverse Transcriptase (Thermo Scientific, Wilmington, DE, USA). The specific DNA fragments for each gene and β-actin were amplified from the mixture solution containing the cDNA template (1 µL), along with 2× Power SYBR Green (6 µL; Toyobo Life Science, Osaka, Japan) and specific primers for FMO3, NKA, AQP5 and FOXA1 genes (Supplementary Table S1) using qRT-PCR. The blanks used a mixture of PCR mixture without cDNA sample. The cycle quantification value (Cq) was calculated using Livak and Schmittgen's method as described in a previous study[48].

Histopathological analysis

To analyze the histopathological structure of sweat gland, the feet tissues were collected from the ICR mice of each group and then fixed in a 10% formalin solution for 48 h. After embedding the trimmed foot tissues in paraffin blocks, the blocks were sectioned into 4 µm thick slices on glass slides. These sections were then stained with a H&E solution (Sigma-Aldrich; Merck KGaA, Darmstadt, Germany), followed by a microscopic examination of the histopathological features, at 400× magnification. The morphological features of these sections were observed using the Leica Application Suite (Leica Microsystems, Herbrugg, Switzerland). The lumen area and secretory coiled portion in the sweat gland were measured using the Image J program 1.52a (NIH, Bethesda, ML, USA) together with Image-Color-Split Channels and the Analysis-Tools-ROI Manager as described in a previous study[51].

Statistical analysis

Statistical analysis between the experimental groups was conducted using One-way Analysis of Variance (ANOVA) (SPSS for Windows, Release 10.10, Standard Version, IL, USA), followed by a Tukey's multiple comparisons test and the independent samples t-test (SPSS for Windows). PCA for multivariate analyses was conducted using SPSS statistics (Release 10.10, Standard Version). All values are presented as the means ± SD, and a $p\text{-value} < 0.05$ was considered significant.

Data availability

All data that support the findings of our data are available from the corresponding author upon reasonable request.

Received: 26 July 2024; Accepted: 23 May 2025
Published online: 01 July 2025

References

1. Mitro, S., Gordon, A. R., Olsson, M. J. & Lundström, J. N. The smell of age: Perception and discrimination of body odors of different ages. *PLoS ONE***7**, e38110. https://doi.org/10.1371/journal.pone.0038110 (2012).
2. Labow, J. N. Human odors. *Perf Flavor.* **4**, 12–17 (1979).
3. Senol, M. & Firman, P. Body odor in dermatological diagnosis. *Cutis* **63**, 107–111 (1999).
4. Wysocki, C. J. & Preti, G. Human body odors and their perception. *Jpn J. Taste Smell* **7**, 19–42 (2000). https://www.researchgate.net/publication/285242523
5. Schaal, B. & Porter, R. H. Microsmatic humans: The generation and perception of chemical signals. In *Advances in the Study of Behavior* (eds Slater, P. J., Rosenblatt, J. S., Beer, C. & Milinski, M.) 135–199 (Academic, Sand Diego, 1991).
6. Gower, D. B. & Ruparelia, B. A. Olfaction in humans with special reference to odorous 16-androstenes: their occurrence, perception, and possible social, psychological and sexual impact. *J. Endocrinol.* **137**, 167–187. https://doi.org/10.1677/joe.0.1370167 (1993).
7. Gallagher, M. et al. Analyses of volatile organic compounds from human skin. *Br. J. Dermatol.* **159**, 780–791. https://doi.org/10.1111/j.1365-2133.2008.08748.x (2008).
8. Haze, S. et al. 2-nonenal newly found in human body odor tends to increase with aging. *J. Invest. Dermatol.* **116**, 520–524. https://doi.org/10.1046/j.0022-202x.2001.01287.x (2001).
9. Natsch, A. What makes us smell: The biochemistry of body odor and the design of new deodorant ingredients. *Chimia (Aarau)* **69**, 414–420. https://doi.org/10.2533/chimia.2015.414 (2015).
10. Lundström, J. N. & Olsson, M. J. Functional neuronal processing of human body odors. *Vitam. Horm.* **83**, 1–23. https://doi.org/10.1016/S0083-6729(10)83001-8 (2010).
11. Song, H. K. & Hwang, D. Y. Use of C57BL/6 N mice on the variety of immunological researches. *Lab. Anim. Res.* **33**, 119–123. https://doi.org/10.5625/lar.2017.33.2.119 (2017).
12. Medetgul-Ernar, K. & Davis, M. M. Standing on the shoulders of mice. *Immunity* **55**, 1343–1353. https://doi.org/10.1016/j.immuni.2022.07.008 (2022).
13. Gervasi, S. S., Opiekun, M., Martin, T., Beauchamp, G. K. & Kimball, B. A. Sharing an environment with sick conspecifics alters odors of healthy animals. *Sci. Rep.* **8**, 14255. https://doi.org/10.1038/s41598-018-32619-4 (2018).
14. Robinson, A. B., Dirren, H. & Sheets, A. Quantitative aging pattern in mouse urine vapor as measured by gas-liquid chromatography. *Exp. Gerontol.* **11**, 11–16. https://doi.org/10.1016/0531-5565(76)90005-x (1976).
15. Osada, K. et al. The scent of age. *Proc. Biol. Sci.* **270**, 929–933. https://doi.org/10.1098/rspb.2002.2308 (2003).
16. Osada, K., Tashiro, T., Mori, K. & Izumi, H. The identification of attractive volatiles in aged male mouse urine. *Chem. Senses.* **33**, 815–823. https://doi.org/10.1093/chemse/bjn045 (2008).
17. Kim, J. E. et al. Evaluation of deodorizing effects of *Saccharina Japonica* in 10-month-dld ICR mice using a novel odor marker associated with aging. *Evid. Based Complement. Alternat Med.* **2022**, 1410144. https://doi.org/10.1155/2022/1410144 (2022).
18. Guo, L. et al. Structural basis of amine odorant perception by a mammal olfactory receptor. *Nature* **618**, 193–200. https://doi.org/10.1038/s41586-023-06106-4 (2023).
19. Gozu, Y. et al. Development of care-products to prevent aged body odor. *J. Soc. Cosmet. Chem. Jpn.* **34**, 379–386. https://doi.org/10.5107/sccj.34.379 (2000).
20. Eriksson, J. G. et al. Higher serum phenylalanine concentration is associated with more rapid telomere shortening in men. *Am. J. Clin. Nutr.* **105**, 144–150. https://doi.org/10.3945/ajcn.116.130468 (2017).
21. Yu, H. T. et al. Untargeted metabolomics approach (UPLC-Q-TOF-MS) explores the biomarkers of serum and urine in overweight/obese young men. *Asia Pac. J. Clin. Nutr.* **27**, 1067–1076. https://doi.org/10.6133/apjcn.052018.07 (2018).
22. Wu, P. H. et al. Exploring the benefit of 2-methylbutyric acid in patients undergoing hemodialysis using a cardiovascular proteomics approach. *Nutrients* **11**, 3033. https://doi.org/10.3390/nu11123033 (2019).
23. Novotny, M. V. et al. Stereoselectivity in mammalian chemical communication: Male mouse pheromones. *Experientia* **51**, 738–743. https://doi.org/10.1007/BF01941272 (1995).
24. Tashiro, T., Osada, K. & Mori, K. Syntheses of 2-Isopropyl-4,5-dihydrothiazole and 6-hydroxy-6-methyl-3-heptanone, pheromone components of the male mouse, *Mus musculus*. *Biosci. Biotechnol. Biochem.* **72**, 2398–2402. https://doi.org/10.1271/bbb.80293 (2008).
25. Novotny, M. V. et al. A unique urinary constituent, 6-hydroxy-6-methyl-3-heptanone, is a pheromonethat accelerates puberty in female mice. *Chem. Biol.* **6**, 377–383. https://doi.org/10.1016/S1074-5521(99)80049-0 (1999).
26. Hartwig, A. & Commission, M. A. K. Trimethylamine [MAK value documentation, 2016]. *E MAK Collect. occup. Health Saf.*. **3**, 1–9 (2018).
27. Falony, G., Vieira-Silva, S. & Raes, J. Microbiology meets big data: The case of gut microbiota-derived trimethylamine. *Annu. Rev. Microbiol.* **69**, 305–321. https://doi.org/10.1146/annurev-micro-091014-104422 (2015).
28. Gaci, N., Borrel, G., Tottey, W., O'Toole, P. W. & Brugere, J. F. Archaea and the human gut: New beginning of an old story. *World J. Gastroenterol.* **20**, 16062–16078. https://doi.org/10.3748/wjg.v20.i43.16062 (2014).
29. Hines, R. N. Developmental and tissue-specific expression of human flavin-containing monooxygenases 1 and 3. *Expert. Opin. Drug Metab. Toxicol.* **2**, 41–49. https://doi.org/10.1517/17425255.2.1.41 (2006).
30. Shehin-Johnson, S. E., Williams, D. E., Larsen-Su, S., Stresser, D. M. & Hines, R. N. Tissue-specific expression of flavin-containing monooxygenase (FMO) forms 1 and 2 in the rabbit. *J. Pharmacol. Exp. Ther.* **272**, 1293–1299 (1995).
31. Koukouritaki, S. B., Simpson, P., Yeung, C. K., Rettie, A. E. & Hines, R. N. Human hepatic flavin-containing monooxygenases 1 (FMO1) and 3 (FMO3) developmental expression. *Pediatr. Res.* **51**, 236–243. https://doi.org/10.1203/00006450-200202000-00018 (2002).
32. Gresham, G. A. & West, I. E. Injury and repair of tracheobronchial cartilage following accidental exposure to ethyleneimine. *J. Clin. Pathol.* **28**, 564–567. https://doi.org/10.1136/jcp.28.7.564 (1975).
33. Carpenter, C. P., Smyth Jr, H. F. & Shaffer, C. B. The acute toxicity of ethylene imine to small animals. *J. Ind. Hyg. Toxicol.* **30**, 2–6 (1948).
34. Santodonato, J., Bosch, S., Meylan, W., Becker, J. & Neal, M. Monograph on human exposure to chemicals in the workplace: Mercaptans. *HERO* **1**, 85–187 (1985).
35. Knudsen, P. Über methylendiamin. *Ber Dtsch. Chem. Ges* **47**, 2698–2701. https://doi.org/10.1002/cber.19140470355 (1914).
36. Galaverna, G., Corradini, R., Dossena, A. & Marchelli, R. Diaminomethane dihydrochloride, a novel reagent for the synthesis of primary amides of amino acids and peptides from active esters. *Int. J. Pept. Protein Res.* **42**, 53–57. https://doi.org/10.1111/j.1399-3011.1993.tb00349.x (1993).
37. Marks, J. H., Wang, J., Fortenberry, R. C. & Kaiser, R. I. Preparation of methanediamine ($CH_2(NH_2)_2$)—A precursor to nucleobases in the interstellar medium. *Proc. Natl. Acad. Sci. USA* **119**, e2217329119. https://doi.org/10.1073/pnas.2217329119 (2022).
38. Cheshire, W. P. & Freeman, R. Disorders of sweating. *Semin Neurol.* **23**, 399–406. https://doi.org/10.1055/s-2004-817724 (2003).

39. Cui, C. Y. & Schlessinger, D. Eccrine sweat gland development and sweat secretion. *Exp. Dermatol.* **24**, 644–650. https://doi.org/10.1111/exd.12773 (2015).
40. Saga, K. Structure and function of human sweat glands studied with histochemistry and cytochemistry. *Prog Histochem. Cytochem.* **37**, 323–386. https://doi.org/10.1016/s0079-6336(02)80005-5 (2002).
41. Diao, J. et al. Sweat gland organoids contribute to cutaneous wound healing and sweat gland regeneration. *Cell. Death Dis.* **10**, 238. https://doi.org/10.1038/s41419-019-1485-5 (2019).
42. Cui, C. Y. et al. Forkhead transcription factor FOXA1 regulates sweat secretion through bestrophin 2 anion channel and Na-K-Cl cotransporter 1. *Proc. Natl. Acad. Sci. USA* **109**, 1199–1203. https://doi.org/10.1073/pnas.1117213109 (2012).
43. Li, H., Chen, L., Zhang, M., Xie, S. & Cheng, L. Expression and localization of forkhead transcription factor A1 in the three-dimensional reconstructed eccrine sweat glands. *Acta Histochem.* **120**, 520–524. https://doi.org/10.1016/j.acthis.2018.06.003 (2018).
44. Song, Y., Sonawane, N. & Verkman, A. S. Localization of aquaporin-5 in sweat glands and functional analysis using knockout mice. *J. Physiol.* **541**, 561–568. https://doi.org/10.1113/jphysiol.2001.020180 (2002).
45. Louie, J. C., Fujii, N., Meade, R. D. & Kenny, G. P. The roles of the Na^+/K^+-ATPase, NKCC, and K^+ channels in regulating local sweating and cutaneous blood flow during exercise in humans in vivo. *Physiol.Rep.* **4**, e13024. https://doi.org/10.14814/phy2.13024 (2016).
46. Callicott, R. J. & Womack, J. E. Real-time PCR assay for measurement of mouse telomeres. *Comp. Med.* **56**, 17–22 (2006).
47. Baek, J. H., Son, H., Jeong, Y. H., Park, S. W. & Kim, H. J. Chronological aging standard curves of telomere length and mitochondrial DNA copy number in twelve tissues of C57BL/6 male mouse. *Cells* **8**, 247. https://doi.org/10.3390/cells8030247 (2019).
48. Livak, K. J. & Schmittgen, T. D. Analysis of relative gene expression data using real-time quantitative PCR and the 2(-delta delta C(T)) method. *Methods* **25**, 402–408. https://doi.org/10.1006/meth.2001.1262 (2001).
49. Kim, J. E. et al. Antioxidant activity and laxative effects of tannin-enriched extract of *Ecklonia cava* in loperamide-induced constipation of SD rats. *PLoS One* **16**, e0246363. https://doi.org/10.1371/journal.pone.0246363 (2021).
50. Brodzik, K., Faber, J., Gotda-Kopek, A. & Łomankiewicz, D. Impact of multisource VOC emission on in-vehicle air quality: Test chamber simulation. *IOP Conf. Ser. Mater. Sci. Eng.* **148**, 012033. https://doi.org/10.1088/1757-899X/148/1/012033 (2016).
51. Concepcion, A. R. et al. Store-operated Ca^{2+} entry regulates Ca^{2+}-activated chloride channels and eccrine sweat gland function. *J. Clin. Invest.* **126**, 4303–4318. https://doi.org/10.1172/JCI89056 (2016).

Acknowledgements

We thank Jin Hyang Hwang, the animal technician, for directing the animal care and use at the Laboratory Animal Resources Center at Pusan National University.

Author contributions

Conceptualization, J.E.K., T.R.K. and D.Y.H.; methodology, J.E.K. and T.R.K.; software, E.S.P, H.J.S. and A.S.; validation, E.S.P. and K.H.P.; formal analysis, J.E.K., T.R.K., H.J.S. and A.S.; investigation, J.E.K. and T.R.K.; resources, S.J.L. and S.H.W.; data curation, J.E.K., T.R.K., S.J.L. and S.H.W.; writing—original draft preparation, D.Y.H.; writing—review and editing, J.E.K. and T.R.K.; visualization, J.E.K. and T.R.K.; supervision, D.Y.H.; project administration, D.Y.H.; funding acquisition, D.Y.H. All authors reviewed the manuscript.

Funding

This work was supported by a National Research Foundation of Korea (NRF) grant funded by the Korean government (MSIT) (No. RS-2023-00211033). Also, this study was supported by the BK21 FOUR project through the National Research Foundation of Korea (NRF) funded by the Ministry of Education, Korea (F24YY8109033). These funders had no role in the design of this study, nor did they have any role during its execution, analyses, interpretation of the data, or decision to submit results.

Declarations

Competing interests

The authors declare no competing interests.

Ethical approval and consent to participate

The animal procedures were approved by the Pusan National University-Institutional Animal Care and Use Committee (PNU-IACUC) based on the ethical procedures for scientific care (Approval Number PNU-2023-0330).

Additional information

Supplementary Information The online version contains supplementary material available at https://doi.org/10.1038/s41598-025-03978-6.

Correspondence and requests for materials should be addressed to D.Y.H.